SN Comprehensive Clinical Medicine (2022) 4:203
https://doi.org/10.1007/s42399-022-01230-0

ORIGINAL PAPER

Iliac Artery Tortuosity, Calcification and Abnormal Shape Augment Aortic Aneurysm Anatomy in Predicting Complications After Endovascular Aneurysm Repair

Alex M. Pagnozzi[1] · Nicholas Dowson[1] · Prue Cowled[2,3] · Benjamin Thurston[3,4] · Robert Fitridge[2,3,4]

Accepted: 29 June 2022 / Published online: 17 September 2022

Abstract

Post-surgical complications following endovascular aneurysm repair (EVAR) remain a risk, arising from technical difficulties imposed by highly calcified or tortuous iliac arteries. Automated methods enable segmentation of the iliac artery to potentially better define perioperative risk prediction. This study uses imaging software to characterise segmental iliac artery anatomy and aims to establish if iliac artery abnormalities can predict adverse outcomes following EVAR. Pre-operative clinical information and CT angiograms were obtained from 189 patients who underwent elective EVAR. Patients were followed for up to 3 years to detect stent-related complications and mortality. Aneurysm morphology was manually measured on CT scans. Automated measurements of vessel shape, curvature and calcification were taken for multiple subdivisions of the common and external iliac arteries. Logistic regression models were trained to assess the influence of iliac artery and aneurysm morphology on outcomes. Combining iliac and aortic features improved predictions of both stent-related complications and morbidity over using either alone. Models predicting death and both early and late stent complications had respective areas under the curve (AUCs) of 0.761, 0.935 and 0.833. Iliac artery calcification and curvature were significant predictors of poor outcomes. Automated morphological assessment of the common and external iliac artery improves the prediction of complications following EVAR. The improved power of iliac morphology to predict late complications and death implies that regional abnormalities of the iliac arteries are important when assessing surgical risk. This allows further rationalisation of the selection of individuals for treatment and may improve patient outcomes.

Keywords Iliac artery · Anatomy · Endovascular · Aneurysm · CT angiogram · Automated analysis

This article is part of theTopical Collection on *Imaging*

✉ Alex M. Pagnozzi
Alex.Pagnozzi@csiro.au

Robert Fitridge
robert.fitridge@adelaide.edu.au

[1] The Australian E-Health Research Centre, CSIRO Health and Biosecurity, Royal Brisbane and Women's Hospital, UQ Health Sciences Building, Level 5, Herston, QLD 4029, Australia

[2] Discipline of Surgery, The University of Adelaide, Adelaide, South Australia 5005, Australia

[3] Discipline of Surgery, The Queen Elizabeth Hospital, 28 Woodville Road, Woodville South, Woodville, South Australia 5011, Australia

[4] Vascular and Endovascular Services, Royal Adelaide Hospital, Port Road, Adelaide, South Australia 5000, Australia

Introduction

Elective endovascular repair of infrarenal aortic aneurysms (EVAR) is now performed more frequently than open repair [1, 2]. Elective EVAR is generally a low-risk procedure, with relatively low morbidity and mortality rates. However, there remain a significant number of post-surgical complications—including early stent-related problems (within 30 days of surgery), later stent-related problems and perioperative death [3]. Some of the stent-related complications may arise from challenging patient anatomy [4], not only of the aorta and aneurysm itself but also of the vessels used to access the aorta. Small, tortuous or calcified iliac arteries may complicate accessing the aneurysm and deploying the stent accurately. The potential risk for early or late limb occlusion is also important to assess.

Previous studies have investigated whether features of the iliac vessels may predict poor outcomes following EVAR. These studies have largely employed manual processes to assess the anatomical features of the iliac artery from pre-operative CT imaging. These techniques often have high inter-observer variability and any relationship between vessel morphology and post-surgical complications has therefore not been clearly demonstrated. In some studies, iliac artery curvature and tortuosity have been found to be correlated with complications after EVAR [5–8]. Similarly, increased systemic arterial calcification burden [9, 10] has been shown to be associated with increased all-cause mortality. Iliac artery calcification was also associated with 12-month all-cause mortality after EVAR [11]. In these studies, iliac tortuosity was examined over the entire length of the artery, while iliac calcification was calculated only from a single cross-sectional image. However, the common and external iliac arteries are not uniform throughout their length and some variation in curvature and diameter is normal. It is likely that unusual curvature or calcification volume in specific regions of the artery may have a greater impact on surgical difficulty than abnormalities in other regions. Indeed, it may be only when abnormal curvature and calcification are co-located at specific discrete locations that difficulties arise. Manual methods that assess the whole iliac artery may therefore lack the resolution to identify concerning morphologies. As a result, the frequency and extent of abnormality in the context of specific location, and their implications for surgical complexity, remain under-explored.

Imaging software is now able to manipulate the pre-operative CT angiogram to perform automatic segmentation and analysis of the iliac arteries [5, 12]. In this study, a novel semi-automated image processing software (Tortuosity in Aorto-Iliac Pathology Nomogram, TAIPAN) was used to quantify the important characteristics of the common and external iliac artery that are indicative of post-EVAR complications. It expands upon our previous study solely characterising tortuosity in the iliac arteries [5], by additionally quantifying calcification burden and atypicality, and including aortic morphology that has been shown to predict adverse outcomes following EVAR [13]. Furthermore, it allows the measurement of these characteristics in specific regions of the artery, as specific regions may have a greater impact on surgical difficulty (such as the stent location). We demonstrate this approach on predicting post-surgical complications following EVAR on a cohort of 189 patients who underwent elective EVAR. This has the potential to rapidly identify patients with abnormal iliac artery anatomy and optimise their pre-operative risk assessment and work-up.

Methods

Data

This study is a retrospective analysis of prospectively collected pre-operative CT angiograms, clinical pre-operative and outcome data from 210 patients undergoing elective EVAR for infrarenal AAAs. Patient enrolment was between 2009 and 2013 across multiple centres including 33 surgeons at 12 public tertiary centres and private hospitals throughout Australia. Ethics approval was obtained from all treating sites, the administering institution (The University of Adelaide), and the Australian Institute of Health and Welfare for the use of national death data. All patients gave informed consent before entering the study.

Using a standardised datasheet and definitions (Supplementary Table), clinical data were obtained from the treating surgeon or a member of their staff before surgery, at 30 days, and 6, 12, 24 and 36 months post-surgery. All-cause mortality information was obtained from the Australian Institute of Health and Welfare National Death Index. Based on how post-EVAR complications are categorised in the clinical setting, outcomes were divided into early graft-related problems (EP) within 30 days of EVAR, which tend to be periprocedural issues such as iliac artery dissection or rupture or issues with stent insertion, deployment and accurate positioning, and late graft-related problems (LP) more than 30 days and within 36 months, which tend to be related to endoleak, limb dislocation, disease progression, stent migration or infection (Table 1). All-cause mortality (> 30 days) was analysed as a separate outcome.

Vessel Modelling

Software

The Tortuosity in Aorto-Iliac Pathology Nomogram (TAIPAN) software [5] was used to segment the common iliac arteries from the contrast-enhanced CT images. CT pre-processing included image de-noising using the anisotropic diffusion algorithm [14], and an exclusion mask to remove cases with extensive streaking artefacts (precluding patients with metal implants). TAIPAN was implemented on a local machine running Ubuntu 16.04, with an 8-core Intel i7 CPU and 24-GB memory and takes on average 235 seconds per patient to run. The segmentations produced by TAIPAN were manually checked to be accurate. The summary of the inputs for TAIPAN, as well as the automated methods and the resulting measures of the iliac artery, is outlined in Fig. 1.

Table 1 Inclusion and exclusion criteria for early graft-related problems (≤ 30 days) and late graft-related problems (> 30 days)

Early graft-related problems (EP)	
Complications at time of procedure and prior to discharge	Inclusions: Operative complications, vessel complications, misplaced deployment, failed deployment, distal embolisation, failed access, twist/kink/obstruction, type 1 endoleak, type 3 endoleak, graft migration, thrombosis, stenosis, graft thrombosis, broken/damaged wires Exclusions: Type 2 endoleak, type 4 endoleak
Unplanned procedures at the time of the operation or prior to discharge for aneurysm or graft	Inclusions: Unplanned procedures pertaining to aneurysm or graft Exclusions: Open groin repair, femoral cut down
Death	Inclusions: Death < 30 days
Late graft-related problems (LP)	
Late post-operative problems	Inclusions: Type 1 or type 3 endoleak, graft kinking, migration, graft thrombosis, broken/damaged wires, graft stenosis Exclusions: Type 2 and type 4 endoleaks
Reoperation for aneurysm	Inclusions: Aneurysm- or graft-related procedure Exclusions: Repairs for type 2 endoleaks (embolisation)
Death	Inclusions: Aneurysm-related (rupture) Exclusions: Death from other causes

Iliac Tortuosity

TAIPAN uses the CT angiograms as well as three manually defined seed points (defined independently by two authors, AP, ND), two in the distal left and right common femoral arteries one slice above the profunda femoris origin and a third seed point 5 mm above the aortic bifurcation, as inputs (Fig. 1). The medial line of the vessel was then found automatically using Dijkstra's algorithm [15], from which vessel curvature (in mm^{-2}) [5], vessel radius (in mm) can also be automatically derived by computing the distance from the medial point to the endothelium in each CT slice.

Iliac Calcification

Calcifications in the vessel (quantified in mL), which appear hyperdense on CT, are also extracted automatically by thresholding the CT images, with a tailored threshold to ensure that non-calcified hyperdensities such as contrast and thrombus were not extracted. Post-processing was performed to extract only those individual calcifications close to the refined iliac vessel mask. Any calcification within this mask was used as input for the statistical models.

Iliac Atypicality and Subdivision

The medial line of the blood vessel was also matched to a population mean vessel of the 189 cases (illustrated in Fig. 1). This was achieved by converting the medial line of the blood vessel into a 2D surface (mesh) format approximating the endothelial surface. The expectation maximisation (EM)-iterative closest point (ICP) [16] was performed by finding the spatial correspondence between each point on each patient's surface mesh and that of the mean of the all the patients (the population mean vessel). The geometric location and scaling of each vessel was then updated to better align with the mean vessel, before correcting the shape of the mean vessel itself. The process is iterated until the mean vessel no longer changes. Using this correspondence to the population mean vessel, the extent of "atypicality" was also quantified (in mm^2), which is the mean Euclidean distance between an individual iliac artery and the population mean vessel (illustrated in Fig. 1). Iliac atypicality complements tortuosity as a measure of challenging iliac anatomy, specifically how much the artery "bows" out laterally. The mean reference vessel was split into either 1, 3, 5 or 10 regions along the length of the common and external iliac arteries, in order to determine what scale of iliac features was most predictive of outcome.

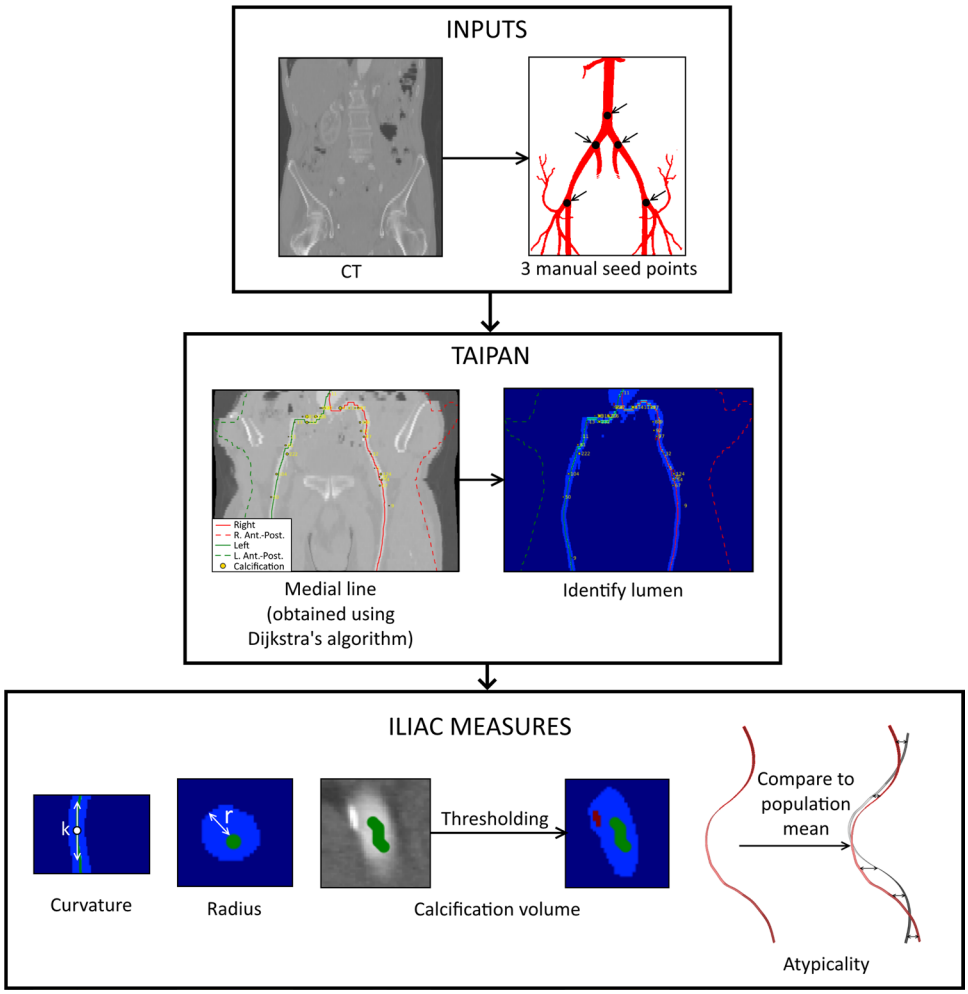

Fig. 1 An illustration of the semi-automated Tortuosity in Aorto-Iliac Pathology Nomogram (TAIPAN) software, including the inputs required by the software (contrast-enhanced CT images and three manual seed points, top box), the automated methods that were used identify the medial line and the lumen of the common iliac arteries (middle box), and the resulting quantitative measures it generates (including curvature of the medial line, vessel radius, volume of calcifications, and atypicality compared to the group mean, bottom box)

Equal divisions of the iliac artery were performed for 5 and 10 regions. For the three-region split ($n=3$), the iliac regions were chosen manually to be on either side of the major bend of the artery. The 1-region split ($n=1$) simply consists of the complete length of the vessel. The subdivisions are illustrated in Fig. 2. The least tortuous vessel (left or right) was used for the purposes of modelling with the more tortuous vessel discarded. Within each region on the iliac arteries, four characteristics were recorded: vessel radius (in mm), mean vessel curvature (in mm^{-2}) [5], the total calcification volume (in mL) and the extent of "atypicality" (in mm^2), which is the mean Euclidean distance between each point of the individuals iliac artery and the population mean vessel of the 189 cases.

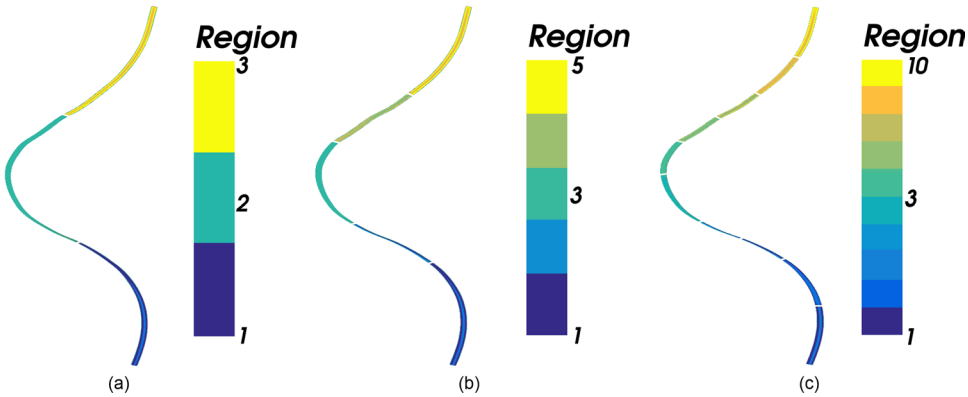

Fig. 2 Illustration of the division of the population mean common iliac artery into (**a**) 3 regions, (**b**) 5 regions and (**c**) 10 regions. All left-hand vessels were mirrored into the right-hand space. The superior-most point corresponds to 5 mm above the aortic bifurcation. The inferior-most points are located in the distal left and right common femoral arteries one slice above the profundal femoris origin

Aortic Features

As aortic features have been found to be predictive of reintervention risks in patients undergoing EVAR [13], a number of aortic features had been quantitatively measured for each patient from the CT by the operating clinician and were available for modelling. These aortic features include the maximum aneurysm diameter, the angle and length of the aortic neck superior to the aneurysm and the aneurysm angle. Definitions of these aortic features, as well as the iliac features, are provided in Table 2. These data were measured on the CT scan by either the treating surgeon or a member of their staff.

Statistical Methodology

The quantitative, regional iliac vessel descriptors and aortic descriptors (Table 2) were used as independent variables in predictive logistic regression models. Patient age and gender, as well as patient comorbidities including the presence of hypertension, diabetes, stroke, renal disease, foot pulse (in either foot) and outcomes from a cardiac assessment, were also included as covariates in the model. First-order linear models were constructed using logistic regression models for each outcome (EP, LP, death) individually, using step-wise variable selection [17] to isolate only the most predictive vessel descriptors. The models were trained on 75% of the data (the training set), allowing the regression coefficients of the most important (i.e. retained) variables to be determined. Applying these coefficients on the remaining 25% of the data (the test set) to obtain estimated outcomes, the classification performance of the fitted models was quantified using the area under the curve (AUC). The AUC measure quantifies the agreement between the model classification and the actual occurrence of post-surgical adverse events, and reflects the generalisability of the model in predicting these clinical outcomes on unseen data. These analyses were performed with the R statistical software version 3.2.2.

Results

Of the 210 CT scans reviewed, 189 segmentations of the iliac artery, their medial lines, vessel radius and calcification location and volume were successfully obtained using TAIPAN. In the remaining 21 cases, CT scans could not be used due to insufficient contrast, or rare cases of extensive streaking artefacts due to metal prostheses. Of the 189 patients with successful analysis of the iliac arteries, 41 had early problems, 33 had late problems, and 63 had either early or late problems (or both). The mean age of the cohort was 75.4 years and all-cause mortality over 36 months was 21% (40 patients). There were 2 perioperative deaths (1%) and aneurysm-related mortality was also low with only two patients (1%) dying from late ruptures. Details of the post-operative and mid-term problems of the final 189 patients are shown in Table 3.

The test set AUCs of the models for EP, LP and death are provided in Table 4. This includes the model constructed using aortic descriptors alone, patient covariates alone, iliac descriptors alone (for all splits of the vessel), and models combining aortic and iliac descriptors with patient covariates. Aortic descriptors alone were found to be predictive of EP (AUC = 0.818), but less predictive of LP and death. Patient covariates (including age, gender, hypertension, diabetes, stroke, renal disease, foot pulse (in either foot) and severity of cardiac disease) were also predictive of all outcomes, particularly of LP (AUC = 0.776). The iliac descriptors alone were mildly predictive of all outcomes, with the best performance occurring for three and five partitions of the iliac for every outcome.

In every case, combining aortic and iliac descriptors with covariates improved predictive performance over either set of descriptors alone (Table 4). For EP, performance peaked using the 1-region model (AUC = 0.935), albeit with the 5-region model giving almost as good performance (AUC = 0.891). For LP, performance was highest for the 3-region model (AUC = 0.833) and for death, the best performance was the 1-region model (AUC = 0.761).

Table 2 Definitions of iliac and aortic features used to predict patient outcomes in the regression models

Iliac features	
Curvature	Mean curvature from each iliac region (in mm^{-2})
Calcification	Total burden from each iliac region (in mL)
Atypicality	Sum of squared distance of iliac region from mean shape of all patients (in mm^2)
Aortic features	
Maximum aneurysm diameter	The maximum diameter of the aortic aneurysm, including the aneurysm wall (in mm)
Infrarenal neck length	Shortest length of the infrarenal neck measured from the lowest renal artery to the beginning of the aneurysm (in mm)
Aortic neck angle	The angle between the axis of the suprarenal aorta and the axis of the aortic neck below the renal arteries (in degrees)
Aneurysm angle	The angle between the axis of the aneurysm neck below the renal arteries and the axis of the aortic sac from commencement of the aneurysm to the aortic bifurcation (in degrees)

Table 3 Summary and incidence of early and late complications after EVAR ($n = 189$ patients)

	Early problems (≤ 30 days)	Late problems (> 30 days)
Renal artery occlusion	2	
Perioperative (≤ 30 days) mortality	2	
Unplanned stent extensions	16	
Type III endoleak	4	
Repair false aneurysm	1	
Failed deployment	1	
Misplaced deployment	2	
Failed access	1	
Type 1 endoleak	9	7
Kinking	1	6
Occlusion	4	5
Stenosis	3	9
Thrombosis	3	12
Renal artery stenosis	1	1
Migration		6
Infolding of graft		1
Type II endoleak with repair		4
Aneurysm-related death > 30 days (rupture)		2

Table 4 The AUCs of the logistic models on the test set, including models consisting of only aortic descriptors, only iliac descriptors (using $n = 1$, 3, 5 and 10 regions), and using both sets of descriptors combined

	EP	LP	Death
Aortic features only	0.818	0.641	0.583
Covariates only	0.692	0.776	0.674
Iliac features only			
1 region	0.710	**0.641**	0.609
3 regions	**0.717**	0.526	**0.630**
5 regions	**0.717**	0.539	0.630
10 regions	0.478	0.487	0.594
Iliac and aortic features and covariates			
1 region	**0.935**	0.641	**0.761**
3 regions	0.705	**0.833**	0.681
5 regions	0.891	0.731	0.725
10 regions	0.536	0.449	0.717

The best performing iliac models are shown in bold

The summary of coefficients for each selected feature in the best performing prediction models is provided in Table 5. The convention in this table is for the first region of the iliac artery to be the most inferior region, with each successively numbered region being more proximal to the aorta. Note in these tables, iliac curvature, calcification volume and distance to the mean shape were computed separately in each iliac region (representing a different variable in the regression model), and only the most predictive regions retained after variable selection are shown in this table. The 10-iliac region models were consistently the worst performing of the models, most likely because the large number of variables relative to the sample size ($n = 189$) resulted in overfitting.

Table 5 The regions from best performing logistic regression models constructed on the train set partition ($n = 142$)

EP		
Variable	Regression coefficient	Standard error
EP		
Aortic neck angle	$-5.767\ 10^{-3}$ *	$2.329\ 10^{-3}$
Aneurysm angle	$7.939\ 10^{-3}$ ***	$2.329\ 10^{-3}$
Age at EVAR	$7.497\ 10^{-3}$	$5.375\ 10^{-3}$
Diabetes	$1.562\ 10^{-1}$	$1.073\ 10^{-1}$
Atypicality—entire iliac length	$-2.328\ 10^{-7}$ **	$8.577\ 10^{-8}$
Calcifications—entire iliac length	$9.485\ 10^{-3}$	$4.943\ 10^{-3}$
LP		
Aneurysm maximum diameter	$7.510\ 10^{-3}$	$4.163\ 10^{-3}$
Aneurysm angle	$3.659\ 10^{-3}$	$2.040\ 10^{-3}$
Age at EVAR	$-1.186\ 10^{-2}$ *	$5.800\ 10^{-3}$
Respiratory assessment	$-8.770\ 10^{-2}$	$5.947\ 10^{-2}$
Foot pulse	−0.166	0.122
Atypicality—2nd region (of 3)	$-1.538\ 10^{-7}$	$8.782\ 10^{-8}$
Curvature—1st region (of 3)	57.13	39.19
Curvature—3rd region (of 3)	35.89 *	15.39
Death		
Aneurysm angle	$3.596\ 10^{-3}$	$1.850\ 10^{-3}$
Age at EVAR	0.021 ***	$5.22\ 10^{-3}$
Hypertension	−0.162	0.093
Stroke	0.348	0.107
Curvature—entire iliac length	−36.07	23.01
Calcifications—entire iliac length	$1.208\ 10^{-3}$ *	$4.66\ 10^{-3}$

Asterisked model correlations were found to be statistically significant: *$p < 0.05$; **$p < 0.01$, ***$p < 0.001$. The iliac regions described in these variables are illustrated in Fig. 1

Atypicality of the entire iliac artery, as well as aneurysm angle and aortic neck angle, was significantly associated with EP, while age at EVAR and curvature in the most inferior portion of the iliac artery were associated with LP. Patient age at EVAR and calcification volume along the entire iliac length were associated with death. Patient age and aneurysm angle were consistently retained factors among all three models, highlighting the importance of these measures for all three outcome types.

Discussion

Our findings show that CT-identified morphological features of the common and external iliac arteries and aorta help predict patients at risk of post-EVAR graft-related adverse events both in the early post-operative period (≤ 30 days) as well as during longer follow-up (> 30 days). Aortic neck angle and aneurysm angle were found to be predictive of early post-EVAR complications, which is consistent with previous findings [18, 19]. Iliac features were also predictive of all post-EVAR complications, and combining aortic and iliac artery features with patient comorbidities led to improvements in predictive power over either set of features alone in every case, suggesting both aortic and iliac anatomy effect surgical risk for individual patients. Moreover, logistic regression revealed that all regions of iliac anatomy were predictive of post-surgical outcome, highlighting the importance assessing regional abnormalities along the whole length of the artery.

Calcification and atypicality across the whole iliac vessel were retained in the model predicting stent-related problems in the first 30 days following EVAR (Table 5), with aortic neck angle and aneurysm angle also being significant predictors as previously described [20, 21]. The relationship of iliac artery calcification to increased early stent-related problems has been thought to be due to the difficulty of obtaining an adequate seal on the distal limb of the endograft in heavily calcified vessels [22] or difficulty delivering the graft into the aorta, particularly if combined with other adverse iliac features.

Fewer aortic and iliac features were found to be significantly associated with later stent-related complications arising more than 30 days after EVAR. Increased curvature in the most proximal segment of the iliac artery when divided into 3 segments was associated with increased risk of late stent complications. This may reflect increased surgical difficulty, as increased tortuosity in this region can complicate deployment of the stent and may lead to kinks or increase the risk of stent migration [18, 23]. However, it is likely that complications occurring due to iliac artery abnormalities occur in the early post-operative period if they are going to happen at all. The only other significant variable was patient age at EVAR, suggesting that age at EVAR may be a marker of poor vascular health and may indicate a reduced ability for the iliac artery to remodel and incorporate the stent.

For mortality, measures across the iliac artery achieved the best performance in predicting death, with total calcification load along the entire artery being significant. The widespread nature of this significant iliac descriptor suggests that death is not linked to procedural complexity, where specific iliac regions may be more important than others. Instead, calcification burden throughout the entire vessel is likely to be an indicator of poor health and hence likelihood of death. Indeed, it is well recognised that arterial calcification is an independent risk factor for both cardiovascular- and non-cardiovascular-related morbidity and mortality [24].

There are several limitations of this study. The limited number of individual complications within the available data (Table 3) meant that it was challenging to identify any particular complication that is affected by altered iliac morphology. However by aggregating these complications into EP, LP and death, the sample size is sufficient to detect general trends across the grouped complications. Also for the present analysis, we have focussed on graft-related complications and have not examined other adverse outcomes that are important in risk stratification, such as post-operative myocardial infarction, renal failure or gastrointestinal problems. Given the low frequency of individual complications following EVAR, a larger study would need to be undertaken to model each of these predictive and outcome variables separately. We do not have a record of which iliac artery was used for the main graft deployment and have presumed it was the least tortuous common iliac artery as default. Finally, although all outputs from the TAIPAN software (calcification volumes and medial lines) were manually checked with the anatomy from the CT image prior to analysis, the software still needs to be validated on different cohorts to ensure its generalisability to new data. As seed points must be manually specified, there would be subtle changes expected if different seed points were chosen by different operators. Once validated, TAIPAN can generate a likelihood (between 0 and 1) of early and late stent-related problems, or mortality, to treating clinicians. This risk assessment can help identify patients who are more likely to have post-EVAR complications and enable appropriate discussion regarding the possible benefit of alternative options for these patients, such as conservative management, delaying EVAR until a larger diameter threshold is reached, consideration of open repair or possibly fenestrated grafting.

Conclusions

In this study, we describe the methods we have developed for automated characterisation of the regional anatomical features of the iliac artery. The correlation between regional iliac artery abnormalities and complications following EVAR was measured, with complications analysed including early stent-related problems (< 30 days post-surgery), late stent-related problems (> 30 days post-surgery) and death. Combining iliac and aortic morphological features consistently improved the ability to predict adverse outcomes over using aortic abnormalities alone. Early problems were

predicted with high accuracy (AUC of 0.935) using a model that incorporated both aortic and iliac features as well as patient covariates, indicating that particular anatomical characteristics of these arteries may impose technical complexity on the EVAR procedure and thus increase early complications. Similarly, iliac and aortic morphological abnormalities correlate with an increased incidence of late graft-related problems and all-cause mortality—although with reduced predictive power for early problems, highlighting the importance of also including non-anatomical risk factors in predicting these outcomes. Overall, we have demonstrated that automated characterisation of the iliac artery is possible and enables specific patient risk to be further refined in the work-up for EVAR. This allows further rationalisation of the selection of treatment and will hopefully improve patient outcomes.

Supplementary Information The online version contains supplementary material available at https://doi.org/10.1007/s42399-022-01230-0.

Author Contribution Alex M. Pagnozzi: methodology, software, validation, formal analysis, visualisation, writing—original draft.

Nicholas Dowson: conceptualisation, methodology, software, supervision, writing—reviewing and editing.

Prue Cowled: data curation, resources, investigation, visualisation, project administration, writing—reviewing and editing.

Benjamin Thurston: conceptualisation, methodology, investigation, writing—reviewing and editing.

Robert Fitridge: conceptualisation, methodology, investigation, project administration, writing—reviewing and editing.

Funding This study was supported by the National Health and Medical Research Council (NHMRC) (project grant number 565335), who provided funding but had no input into study design, data collection, analysis and interpretation of data and in writing the manuscript.

Data Availability According to the study ethics from the Queen Elizabeth Hospital (Application number 2008162), this data is not to be made available to a third party. As a result of these ethics, making these data accessible to a third party will require new ethical approval to be sought. As CI of the study, Robert Fitridge (robert.fitridge@adelaide.edu.au) would be the contact for whom any request for data access may be submitted.

Code Availability The TAIPAN code is not publicly available.

Declarations

Ethics Approval All procedures performed in studies involving human participants were in accordance with the ethical standards of the institutional and national research committees and with the 1964 Helsinki Declaration and its later amendments or comparable ethical standards.

Consent to Participate Informed Consent was obtained from all individual participants included in the study.

Consent for Publication Consent to publish was obtained from all individual participants included in the study.

Conflict of Interest The authors declare no competing interests.

References

1. Sethi RKV, Henry AJ, Hevelone ND, Lipsitz SR, Belkin M, Nguyen LL. Impact of hospital market competition on endovascular aneurysm repair adoption and outcomes. J Vasc Surg. 2013;58:596–606.
2. Beck AW, Sedrakyan A, Mao J, Venermo M, Faizer R, Debus S, et al. Variations in abdominal aortic aneurysm care: a report from the International Consortium of Vascular Registries. Circulation. 2016;134:1948–58.
3. Barnes M, Boult M, Maddern G, Fitridge R. A model to predict outcomes for endovascular aneurysm repair using preoperative variables. Eur J Vasc Endovasc Surg. 2008;35:571–9.
4. Schanzer A, Messina L. Two decades of endovascular abdominal aortic aneurysm repair: enormous progress with serious lessons learned. J Am Hear Assoc Cardiovasc Cerebrovasc Dis [Internet]. Wiley-Blackwell; 2012 [cited 2022 May 23];1. Available from:https://www.com/pmc/articles/PMC3487335.
5. Dowson N, Boult M, Cowled P, De Loryn T, Fitridge R. Development of an automated measure of iliac artery tortuosity that successfully predicts early graft-related complications associated with endovascular aneurysm repair. Eur J Vasc Endovasc Surg WB Saunders Ltd. 2014;48(153):60.
6. Ueda T, Takaoka H, Raman B, Rosenberg J, Rubin GD. Impact of quantitatively determined native thoracic aortic tortuosity on endoleak development after thoracic endovascular aortic repair. Am J Roentgenol American Roentgen Ray Society. 2011;197(1140):6.
7. Coulston J, Baigent A, Selvachandran H, Jones S, Torella F, Fisher R. The impact of endovascular aneurysm repair on aortoiliac tortuosity and its use as a predictor of iliac limb complications. J Vasc Surg. 2014;60:585–9.
8. Kyriakou F, Dempster W, Nash D. A methodology to quantify the geometrical complexity of the abdominal aortic aneurysm. Sci Reports 2019 91 [Internet]. Nature Publishing Group; 2019 [cited 2022 May 23];9:1–12. Available from: https://www.nature.com/articles/s41598-019-53820-z.
9. Mori H, Torii S, Kutyna M, Sakamoto A, Finn AV, Virmani R. Coronary artery calcification and its progression: what does it really mean? JACC Cardiovasc Imaging Elsevier. 2018;11:127–42.
10. Madhavan MV, Tarigopula M, Mintz GS, Maehara A, Stone GW, Généreux P. Coronary artery calcification: pathogenesis and prognostic implications. J Am Coll Cardiol 2014;6:1703–14. Available from: https://pubmed.ncbi.nlm.nih.gov/24530667/.

11. Fitridge RA, Boult M, De Loryn T, Cowled P, Barnes M. Predictors of 1-year survival after endovascular aneurysm repair. Eur J Vasc Endovasc Surg WB Saunders Ltd. 2016;51(528):34.
12. Lalys F, Yan V, Kaladji A, Lucas A, Esneault S. Generic thrombus segmentation from pre- and post-operative CTA. Int J Comput Assist Radiol Surg. 2017
13. Karthikesalingam A, Attallah O, Ma X, Bahia SS, Thompson LL, Vidal-Diez A, Choke EC, Bown MJ, Sayers RD, Thompson MM, Holt PJ. An artificial neural network stratifies the risks of reintervention and mortality after endovascular aneurysm repair; a retrospective observational study. Kirchmair R, editor. PLoS One. 2015;10:e0129024. https://doi.org/10.1371/journal.pone.0129024.
14. Osher S, Sethian JA. Fronts propagating with curvature-dependent speed: algorithms based on Hamilton-Jacobi formulations. J Comput Phys. 1988;79:12–49.
15. Dijkstra EW. A note on two problems in connexion with graphs. Numer Math Springer-Verlag. 1959;1:269–71.
16. Shen K, Bourgeat P, Fripp J, Meriaudeau F, Salvado O. Consistent estimation of shape parameters in statistical shape model by symmetric EM algorithm. Proc SPIE 8314, Med Imaging 2012 Image Process. 83140R. 2012. Available from https://doi.org/10.1117/12.911746.
17. Sugiura N. Further analysts of the data by Akaike's information criterion and the finite corrections. Commun Stat - theory methods. Marcel Dekker, Inc.;7:13–26.
18. Wyss TR, Dick F, Brown LC, Greenhalgh RM. The influence of thrombus, calcification, angulation, and tortuosity of attachment sites on the time to the first graft-related complication after endovascular aneurysm repair. J Vasc Surg. 2011;54:965–71.
19. Stather PW, Wild JB, Sayers RD, Bown MJ, Choke E. Endovascular aortic aneurysm repair in patients with hostile neck anatomy. J Endovasc Ther [Internet]. SAGE PublicationsSage CA: Los Angeles, CA; 2013 [cited 2022 May 23];20:623–37. Available from: https://journals.sagepub.com/doi/abs/10.1583/13-4320MR.1.
20. Bastos Gonçalves F, De Vries JPPM, Van Keulen JW, Dekker H, Moll FL, Van Herwaarden JA, et al. Severe proximal aneurysm neck angulation: early results using the Endurant Stentgraft System. Eur J Vasc Endovasc Surg [Internet]. Elsevier; 2011 [cited 2022 May 23];41:193–200. Available from: http://www.ejves.com/article/S1078588410006787/fulltext.
21. Bryce Y, Rogoff P, Romanelli D, Reichle R. Endovascular repair of abdominal aortic aneurysms: vascular anatomy, device selection, procedure, and procedure-specific complications. [Internet]. Radiological Society of North America ; 2015 [cited 2022 May 23];35:593–615. Available from: https://doi.org/10.1148/rg.352140045.
22. Buijs RVC, Willems TP, Tio RA, Boersma HH, Tielliu IFJ, Slart RHJA, et al. Calcification as a risk factor for rupture of abdominal aortic aneurysm. Eur J Vasc Endovasc Surg [Internet]. Elsevier; 2013 [cited 2022 May 23];46:542–8. Available from: http://www.ejves.com/article/S1078588413005686/fulltext.
23. Dillavou ED, Muluk SC, Rhee RY, Tzeng E, Woody JD, Gupta N, et al. Does hostile neck anatomy preclude successful endovascular aortic aneurysm repair? J Vasc Surg. 2003;38:657–63.
24. Allison MA, Hsi S, Wassel CL, Morgan C, Ix JH, Wright CM, et al. Calcified atherosclerosis in different vascular beds and the risk of mortality. Arterioscler Thromb Vasc Biol. 2012;32:140–6.